DOI: 10.61782/fa.2025.0833

STREAMLINING UNDERWATER ACOUSTIC PROPAGATION MODELING WITH A PYTHON-BASED INTERFACE

Ion Urtiaga Chasco[1*] **Alonso Hernández Guerra**[1]

[1] Instituto de Oceanografía y Cambio Global, Universidad de Las Palmas de Gran Canaria, Spain

ABSTRACT

Understanding underwater acoustic propagation is essential for assessing the potential impacts of anthropogenic noise on marine ecosystems. The Ocean Acoustics Library (OALIB, U.S. Office of Naval Research, Ocean Acoustics Program; https://oalib-acoustics.org/) provides valuable tools for characterizing underwater noise. Two widely accepted models are Bellhop and the Range-Dependent Acoustic Model (RAM). These models, which are Fortran-based, use ray-tracing techniques and parabolic equations, respectively, to estimate transmission losses between the source and the receiver. However, these models have different input file formats and require considerable time and effort to configure according to their specifications.

To address these challenges, we are developing an integrated Python-based software solution that enables users to easily set input parameters (e.g., source and receiver positions, propagated noise characteristics, frequency, and source level) and run the Bellhop and RAM models. This integration facilitates simultaneous computation of noise propagation from multiple sources and frequencies, allowing the estimation of Sound Pressure Level (SPL) spectrograms at target locations in a user-friendly manner. Additionally, we are testing graphical user interfaces (GUIs) such as Tkinter, which could further simplify the application of these algorithms.

The ultimate goal of this development is to make noise propagation modeling more accessible to the scientific community, bridging the gap between noise generation and its environmental repercussions.

*__*Corresponding author*__: *ion.urtiaga@ulpgc.es.*

Keywords: *Underwater Acoustic Propagation, Noise Modeling, Python Integration, Marine Ecosystems Impact*

1. INTRODUCTION

Underwater anthropogenic noise impacts aquatic ecosystems and can cause permanent, irreversible damage to a wide range of species. The rise in vessel traffic, driven by industrial advancements and increasing global demand, along with the expansion of ocean-based energy solutions such as offshore wind farms [1], has led to a significant increase in noise levels emitted into the oceans. To understand the effect of anthropogenic noise in the oceans, it is essential to study how the sound propagates from the source to the surrounding environment. In the sea, the sound travels as a pressure p-wave [2], which experience reflection and refraction phenomena in travel due to the vertical seawater stratification. Schematically, a ray theory approach gives us the relationship between the sound speed (related to the stratified sea water density) and the ray angle.

$$\frac{\cos\theta}{c} = \text{constant} \tag{1}$$

Where θ is the launching angle of the ray at a specific position, and c represents the sound speed at this position. This implies that the sound is trapped in the sea within minimum speed zones [2]. In the same way, the sound in the seawater is attenuated by scattering processes and water particle absorption where it is transformed into heat. On the other hand, the bottom-seafloor and atmosphere-ocean interface are complex boundaries that interact with the transferring sound. Thus, knowing the geo-acoustic behavior of these boundaries, together with the seawater characteristics, is essential to study sound propagation. Underwater acoustic propagation has been described by several models, responding to different environmental and source characteristics. Table 1 summarizes the main ocean acoustic propagation models, underlining some of their features and requirements. As the computational cost limits some of these methods (Deveau, 2015) [3], the Ray Model and the Parabolic wave Equations (PE) are the two most commonly used models. They also have the advantage of considering range-varying environments (environments whose acoustic characteristics, such as the sound speed vertical profile or the bathymetry, change with the distance to the source). Additionally, PE allows us to calculate the superposition effect of sound compressional p-waves and shear s-waves [4].

In this study we aim to develop an integrated underwater noise propagation modeling software. The most efficient way to reach this purpose is integrating the already existing and fortran based Ray Tracing model (Bellhop, Porter, 2011) and Parabolic Equation model (Range Dependent Acoustic Model, RAM, Collins, 1995) in a Python script. To test the developed software, we analyze two different study cases corresponding to Gran Canaria to Tenerife channel and to the Gulf of Venice Shallow waters.

2. DATA AND METHODS

Both used propagation software are available at the Ocean Acoustics Library (OALIB,U.S. Office of Naval Research, Ocean Acoustics Program). To calculate the sound propagation in the sea, it is necessary to obtain the underwater sound speed (c). It is known that the sound speed in the ocean is related to sea-water density and can be described by an empirical increasing function depending on the in situ IPTS-68 temperature (T) in degrees Celsius, salinity PSS-68 (S) in parts per thousand, and depth (z) in meters [5].

$$c = 1449.2 + 4.6T - 0.055T^2 + 0.00029T^3 \\ + (1.34 - 0.01T)(S - 35) + 0.016z \tag{2}$$

We use sea water temperature and salinity from the Copernicus Marine Service´s Global Ocean Physics Reanalysis product [6].

To perform the propagation it is also required to accurately describe the geo-physical environment characteristics. In this study, we have analyzed two study cases, one in Gran Canaria to Tenerife channel deep waters, and the other in the Gulf of Venice shallow waters. We have compared several bathymetry repositories, looking for the best resolution. Emodnet product offers the highest resolution and is downloaded from . In the model setup, a single sediment layer has been assumed. The geoacoustic characteristics of seabed sediments are summarized in [7]. These results are schematized in [2] for various common seabed materials and can, therefore, be incorporated into the propagation model. We have integrated in a python

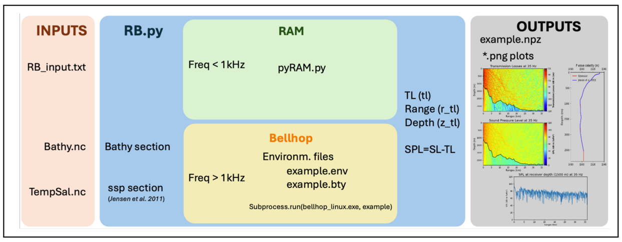

Figure 1. Working scheme of RAM-Bellhop python script, together with its inputs/outputs.

script, several tools that from common inputs, generate several usefull datasets (Figure 1). Firstly, the user sets the desired input parameters (name, locations, frequency,. . .). The program uses this inputs and the bathymetry, temperature and salinity netCDF files to extract the corresponding source-to-receiver sections. The sound speed profile (SSP) is estimated as [5]. Once the source-to-receiver bathymetry and SSP sections are created, the program estimates the Transmission Losses (TL) section. For this purpose, RAM or Bellhop models are used for frequencies below or above 1kHz, respectively. The Sound Pressure Level is later estimated using the sonar equation:

$$SPL = SL - TL \tag{3}$$

where SPL is the sound pressure level expressed in dB re 12, SL represents the Source Level in dB re 12 @ 1m, and TL is the transmission loss in dB re 1m.

To integrate the models, we used pyRAM (Donnelly, 2017), a Python adaptation of RAM; Bellhop (Porter, 2005), compiled from its original Fortran version on Ubuntu; and Arlpy (Chitre, 2020), which processes Bellhop's .shd output via the compute_transmission_loss function.

3. STUDY CASES

To test the propagation program under different conditions, we computed two sections. First, the Tenerife

Table 1. Underwater acoustic propagation models summary. Abbreviations d, r, f and stand for the environment depth, the range or distance to the source, the sound wave frequency and its wavelength, respectively. The frequency limit values are indicative, and they depend on the environmental characteristics and complexity of the input data.

Model	**Equations**	**Range dependence**	**Computational requirements**
Ray Models	Snell-Descartes. Beam tracing	Yes	$d \gg \lambda$
Normal Modes	Stationary waves	No	Low f and d
Parabolic Wave Equation (PE)	Helmholtz approximation	Yes	$r \gg \lambda$; $f < 2kHz$
Fast Field Program (FFP)	Exact environment calculation	No	low r; $f < 1kHz$
Finite Differences/Elements (FD/FE)	Wave equation in segmented regions	Yes	Very low r

to Gran Canaria (Spain) deep waters channel; and second, the Gulf of Venice (Italy) shallow waters. We considered the same frequencies, Source Levels (SL), and seabed geoacoustic characteristics for comparison. For both cases, we propagated the source noise frequencies and Source Levels from [8]. These correspond to the noise generated by a fixed 3.6 MW monopile turbine.

In this study, we used a 10 to 14 m/s wind speed spectrum. As the hydrophone in [8] was located 50 m from the source, we computed back-propagation following [9]. We estimated transmission loss (TL) between the source and receiver on the measurement date using the RAM and Bellhop models. We determined the Source Level (SL) by adding the recorded sound pressure level (SPL) at the hydrophone position to the TL between the source and the hydrophone. The resulting overall SL for the most intense frequencies was 150 dB re 1 $\mu Pa@1m$.

We considered Basalt geoacoustic properties for the bottom description. We used temperature and salinity data from 2019-09-16 to calculate the SSP at each analyzed section.

3.1 Gran Canaria – Tenerife (Deep waters)

In this section, the source and receiver were positioned to reach the deep waters of the Tenerife to Gran Canaria channel. The noise source is 500 m deep at 28.5ºN, 16.1ºW, and the receiver is 1500 m deep at 28.2ºN, 16.0ºW. Figure 2 shows the bathymetry map with the source and receiver positions. The plotted SSP corresponds to the profile with the deepest available temperature and salinity data within the source-to-receiver section. In this case, the deepest SSP profile (Figure 2b) didn't reach depths under 2500, so the program repeated the 2500m deep P-wave celerity value until the bottom.

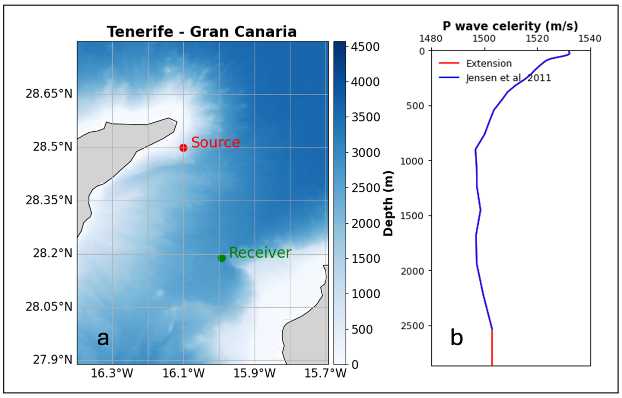

Figure 2. (a) Bathymetry map of Tenerife-Gran Canaria deep water study case. (b) Deepest sound speed profile from the section between the source and receiver shown in the map.

Figure 3 shows the Sound Pressure Level section, calculated with RAM and using range and depth steps of 10 m (left) and 5 m (right). when frequency increases, the SPL differences between 10 m and 5 m calculation steps grow. Thus, higher frequencies require shorter steps. Figure 8 presents a main sound beam reflecting on the surface near 5 km ranges and reaching the seabed at 25 to 30 km. Figure 4 represents the SPL section estimated with

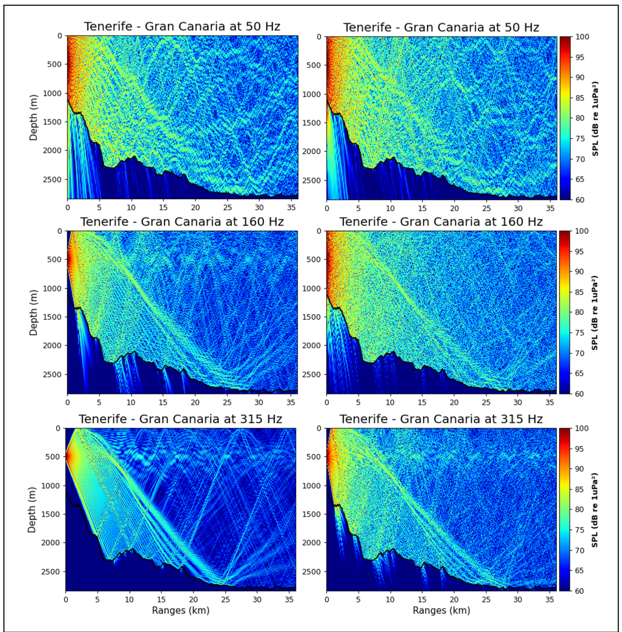

Figure 3. Sound Pressure Level (SPL) sections from Tenerife-Gran Canaria deep water study case, at increasing frequencies (from top to bottom), calculated with RAM model using 10 m (left) and 5 m (right) range and depth steps.

Bellhop, using launching angles of ± 45º (left) and ± 90º (right), at 1100Hz frequency. It shows that significant differences in SPL are only appreciable in near-source ranges (5 km). The surface-seabed reflected beam seen in RAM SPL sections can also be found in this ray-tracing solution.

3.2 Gulf of Venice (Shallow waters)

In this case, the noise source was positioned 5 m deep at 43.36ºN and 12.46ºE, and the receiver was located 10 m deep at 45.10ºN, 13.08ºE. The corresponding Sound speed Profile (SSP), and bathymetry map with source and receiver positions are shown in Figure 10. At such shal-

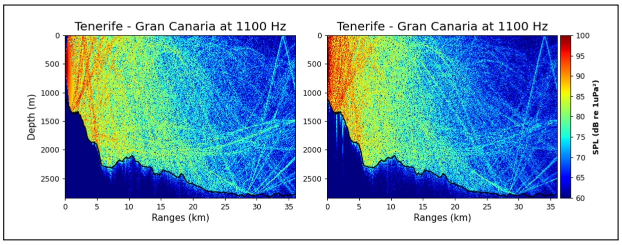

Figure 4. Sound Pressure Level (SPL) sections from Tenerife-Gran Canaria deep water study case, at increasing frequencies (from top to bottom), calculated with the Bellhop model using ± 45º (left) and ± 90º (right) launching angles.

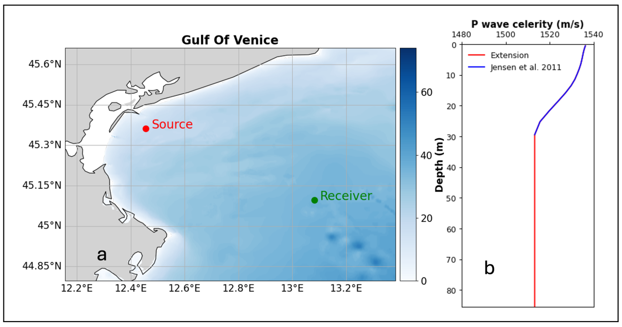

Figure 5. As in figure 2, but for the Gulf of Venice.

low depths, the SSP barely reaches the thermocline (Figure 10b), and therefore, the deepest value was repeated until the bottom. For TL calculation, the depth steps of the RAM model were reduced from 10 m (left) to 0.5 m (right), while maintaining a range step of 10 m. With a 10 m depth calculation step, the 50 m deep section shows an irregular grid, with an unrealistic shape. Using a 0.5 m depth step, the sound propagates towards almost 60 km, keeping a high SPL caused by the continuous reflection between the surface and the seabed. Besides, SPL decreases as frequency and range increase.

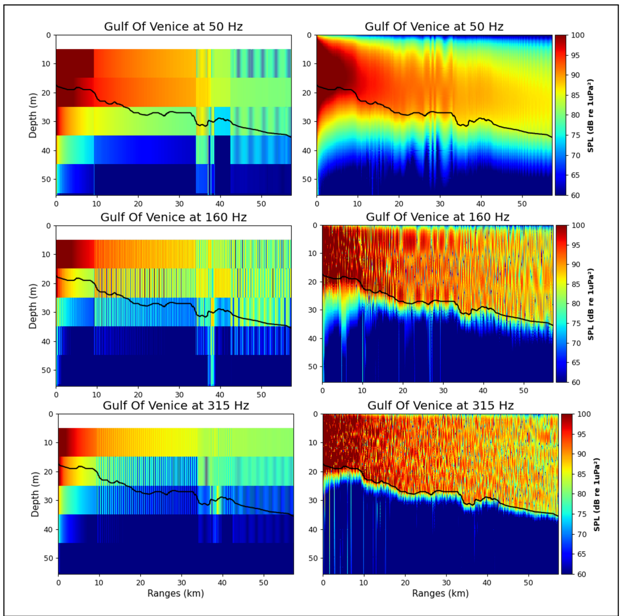

Figure 6. As in figure 3, but for the Gulf of Venice.

In Figure 7 no significant improvements are observed when using ± 90º launching angles. However, Bellhop´s solution shows a noticeably lower underwater SPL and a higher SPL in the seabed than RAM.

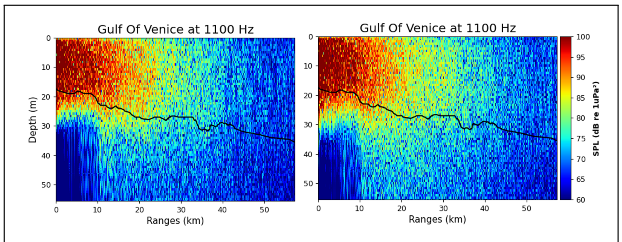

Figure 7. As in figure 3, but for the Gulf of Venice.

4. CONCLUSSIONS

Underwater acoustic propagation programs are often not intuitive and vary widely in their approaches. Our goal is to integrate several of these tools into a unified Python script that we are currently developing. We have tested two case studies—one in shallow water and one in deep water—with promising results in terms of both efficiency and resolution. Currently, we are working on incorporating multi-source and full-spectrum noise propagation. Additionally, we are considering the development of a user-friendly interface within a Jupyter Notebook environment.

5. ACKNOWLEDGMENTS

I extend my gratitude to Adrian Vega Morales (ULPGC) for assistance in migrating the propagation software from Windows to Ubuntu and transitioning from Matlab to Python.

6. REFERENCES

[1] J. Tougaard, L. Hermannsen, and P. T. Madsen, "How loud is the underwater noise from operating offshore wind turbines?," *The Journal of the Acoustical Society of America*, vol. 148, pp. 2885–2893, Nov. 2020. Number: 5.

[2] F. B. Jensen, W. A. Kuperman, M. B. Porter, and H. Schmidt, *Computational Ocean Acoustics*. Modern Acoustics and Signal Processing, New York, NY: Springer New York, 2011.

[3] T. J. Deveau, "A TOOLSET FOR MODELLING ANTHROPOGENIC UNDERWATER NOISE,"

[4] M. D. Collins, "Applications and time-domain solution of higher-order parabolic equations in underwater acoustics," *The Journal of the Acoustical Society of America*, vol. 86, pp. 1097–1102, Sept. 1989. Number: 3.

[5] H. Medwin, "Speed of sound in water: A simple equation for realistic parameters," *The Journal of the Acoustical Society of America*, vol. 58, pp. 1318–1319, Dec. 1975.

[6] M. Drévillon, J.-M. Lellouche, C. Régnier, G. Garric, C. Bricaud, and R. Bourdallé-Badie, "Global Ocean Reanalysis Products GLOBAL_reanalysis_phy_001_030," no. 1, 2023.

[7] E. L. Hamilton, “Sound velocity–density relations in sea-floor sediments and rocks,” *The Journal of the Acoustical Society of America*, vol. 63, pp. 366–377, Feb. 1978. Number: 2.

[8] T. Pangerc, P. D. Theobald, L. S. Wang, S. P. Robinson, and P. A. Lepper, “Measurement and characterisation of radiated underwater sound from a 3.6 MW monopile wind turbine,” *The Journal of the Acoustical Society of America*, vol. 140, pp. 2913–2922, Oct. 2016. Number: 4.

[9] F. Pace, R. D. J. Burns, S. B. Martin, M. A. Wood, C. C. Wilson, C. E. Lumsden, K. M. Murvoll, and J. Weissenberger, “Underwater Sound Emissions from the Moorings of Floating Wind Turbines: HYWIND Scotland Case Study,” in *The Effects of Noise on Aquatic Life* (A. N. Popper, J. Sisneros, A. D. Hawkins, and F. Thomsen, eds.), pp. 1–23, Cham: Springer International Publishing, 2024.